Biomedical Optics EXPRESS

On-chip laser Doppler vibrometer for arterial pulse wave velocity measurement

Yanlu Li,[1,2,*] **Patrick Segers,**[3] **Joris Dirckx,**[4] **and Roel Baets**[1,2]

[1]*Photonics Research Group, INTEC-department, Ghent University-IMEC, Sint-Pietersnieuwstraat 41, 9000, Ghent, Belgium*
[2]*Center for Nano- and Biophotonics (NB-Photonics), Ghent University, Sint-Pietersnieuwstraat 41, 9000, Ghent, Belgium*
[3]*IBiTech-bioMMeda, Ghent University, De Pintelaan 185, 9000 Ghent, Belgium*
[4]*Laboratory of Biomedical Physics, University of Antwerp, Groenenborgerlaan 171, 2020 Antwerp, Belgium*
[*]*Yanlu.Li@intec.ugent.be*

Abstract: Pulse wave velocity (PWV) is an important marker for cardiovascular risk. The Laser Doppler vibrometry has been suggested as a potential technique to measure the local carotid PWV by measuring the transit time of the pulse wave between two locations along the common carotid artery (CCA) from skin surface vibrations. However, the present LDV setups are still bulky and difficult to handle. We present in this paper a more compact LDV system integrated on a CMOS-compatible silicon-on-insulator substrate. In this system, a chip with two homodyne LDVs is utilized to simultaneously measure the pulse wave at two different locations along the CCA. Measurement results show that the dual-LDV chip can successfully conduct the PWV measurement.

OCIS codes: (280.3340) Laser Doppler velocimetry; (130.6750) Systems.

References and links

1. Reference Values for Arterial Stiffness' Collaboration, "Determinants of pulse wave velocity in healthy people and in the presence of cardiovascular risk factors: 'establishing normal and reference values'," Eur. Heart J. **31**(19), 2338–2350 (2010).
2. L. M. Van Bortel, S. Laurent, P. Boutouyrie, P. Chowienczyk, J. K. Cruickshank , T. De Backer, J. Filipovsky, S. Huybrechts, F. U. Mattace-Raso, A. D. Protogerou, G. Schillaci, P. Segers, S. Vermeersch, and T. Weber, "Expert consensus document on the measurement of aortic stiffness in daily practice using carotid-femoral pulse wave velocity," J. Hypertens. **30**(3), 445–448 (2012).
3. A. Campo, P. Segers, and J. Dirckx, "Laser Doppler vibrometry for in vivo assessment of arterial stiffness," IEEE International Workshop on Medical Measurements and Applications Proceedings 11 (2011).
4. M. W. Rajzer, W. Wojciechowska, M. Klocek, I. Palka, M. Brzozowska-Kiszka, and K. Kawecka-Jaszcz, "Comparison of aortic pulse wave velocity measured by three techniques: Complior, SphygmoCor and Arteriograph," J. Hypertens. **26**(10), 2001–2007 (2008).
5. G. Mancia, G. De Backer, A. Dominiczak, R. Cifkova, R. Fagard, G. Germano, G. Grassi, A. M. Heagerty, S. E. Kjeldsen, S. Laurent, K. Narkiewicz, L. Ruilope, A. Rynkiewicz, R. E. Schmieder, H. A. Boudier, A. Zanchetti, A. Vahanian, J. Camm, R. De Caterina, V. Dean, K. Dickstein, G. Filippatos, C. Funck-Brentano, I. Hellemans, S. D. Kristensen, K. McGregor, U. Sechtem, S. Silber, M. Tendera, P. Widimsky, J. L. Zamorano, S. Erdine, W. Kiowski, E. Agabiti-Rosei, E. Ambrosioni, L. H. Lindholm, M. Viigimaa, S. Adamopoulos, E. Agabiti-Rosei, E. Ambrosioni, V. Bertomeu, D. Clement, S. Erdine, C. Farsang, D. Gaita, G. Lip, J. M. Mallion, A. J. Manolis, P. M. Nilsson, E. O'Brien, P. Ponikowski, J. Redon, F. Ruschitzka, J. Tamargo, P. van Zwieten, B. Waeber, and B. Williams, "2007 Guidelines for the management of arterial hypertension. The

#190785 - $15.00 USD Received 17 May 2013; revised 18 Jun 2013; accepted 18 Jun 2013; published 27 Jun 2013

task force for the management of arterial hypertension of the European Society of Hypertension (ESH) and the European Society of Cardiology (ESC)," Eur. Heart J. **28**(12), 1462–1536 (2007).
6. E. Hermeling, K. D. Reesink, R. S. Reneman, and A. P. G. Hoeks, "Confluence of incident and reflected waves interferes with systolic foot detection of the carotid artery distension waveform," J. Hypertens. **26**(12), 2374–2380 (2008).
7. J. Luo, R. X. Li, and E. E. Konofagou, "Pulse wave imaging of the human carotid artery: an in vivo feasibility study," IEEE Trans. Ultrason. Ferr. **59**(1), 174–181 (2012).
8. A. Campo and J. Dirckx, "Dual-beam laser Doppler vibrometer for measurement of pulse wave velocity in elastic vessels," 22nd Congress of the International Commission for Optics: Light for the Development of the World **8011**, 80118Y-1 (2011).
9. Y. Li and R. Baets, "Homodyne laser Doppler vibrometer on silicon-on-insulator with integrated 90 degree optical hybrids," Opt. Express **21**(11), 13342–13350 (2013).
10. G. Giuliani, M. Norgia, S. Donati, and T. Bosch, "Laser diode self-mixing technique for sensing applications," J. Opt. A—Pure Appl. Opt. **4**(6), S283–S294 (2002).
11. W. Bogaerts, R. Baets, P. Dumon, V. Wiaux, S. Beckx, D. Taillaert, B. Luyssaert, J. Van Campenhout, P. Bienstman, and D. Van Thourhout, "Nanophotonic waveguides in Silicon-on-Insulator fabricated with CMOS Technology," J. Lightwave Technol. **23**(1), 401–412 (2005).
12. N. A. Yebo, S. P. Sree, E. Levrau, C. Detavernier, Z. Hens, J. A. Martens, and R. Baets, "Selective and reversible ammonia gas detection with nanoporous film functionalized silicon photonic micro-ring resonator," Opt. Express **20**(11), 11855–11862 (2012).
13. S. Stankovic, R. Jones, M. N. Sysak, J. M. Heck, G. Roelkens, and D. Van Thourhout, "Hybrid III-V/Si distributed feedback laser based on adhesive bonding," IEEE Photon. Technol. Lett. **24**(23), 2155–2158 (2012).
14. L. Vivien, J. Osmond, J.-M. Fédéli, D. Marris-Morini, P. Crozat, J.-F. Damlencourt, E. Cassan, Y. Lecunff, and S. Laval, "42 GHz p.i.n Germanium photodetector integrated in a silicon-on-insulator waveguide," Opt. Express **17**(8), 6252–6257 (2009).
15. R. Halir, G. Roelkens, A. Ortega-Moñux, and J. G. Wangüemert-Pérez, "High-performance 90° hybrid based on a silicon-on-insulator multimode interference coupler," Opt. Lett. **36**, 178–180 (2011).
16. Y. Li, S. Verstuyft, G. Yurtsever, S. Keyvaninia, G. Roelkens, D. Van Thourhout, and R. Baets, "Heterodyne laser Doppler vibrometers integrated on silicon-on-insulator based on serrodyne thermo-optic frequency shifters," Appl. Opt. **52**, 2145-2152 (2013).
17. http://www.epixfab.eu

1. Introduction

Pulse wave velocity (PWV) is an important measure for arterial stiffness, which is highly related with many cardiovascular diseases. A larger value of PWV indicates a greater arterial stiffness and thus a higher risk of cardiovascular events, so in clinical practice PWV is used as an important and independent predictor of cardiovascular mortality [1–4]. In practice, the carotid-femoral PWV, which describes the average velocity of the arterial pulse propagating from the carotid to the femoral artery, is usually used. The European Society of Hypertension suggested that a carotid-femoral PWV of 12 m/s can be considered as the threshold of an estimate of subclinical organ damage [5], and individuals with a carotid-femoral PWV higher than this threshold should seek for clinical treatments to prevent cardiovascular events.

Several devices have been introduced to measure the carotid-femoral PWV, the most well known being the Complior and Sphygmocor system [4]. For the assessment of local arterial PWV, however, there are no widespread commercial devices. It is only since recent that efforts have been undertaken to measure the propagation of the pulse using fast ultrasound-based techniques [6, 7]. Additionally, the measurement setup of the carotid-femoral PWV is usually bulky and sometimes causes discomfort to subjects because they are palpated in the groin. A new noninvasive method to measure the local PWV of the common carotid arteries (CCAs) using laser Doppler vibrometry (LDV) technique has been proposed [3, 8]. This method simplifies the measurement procedures and also overcomes the uneasiness in the conventionally used carotid-femoral PWV measurement. However, the proposed measurement setup for the CCA PWV measurement is still bulky, which prevent this technique from being widely used.

In this paper, we present a compact device for the CCA PWV measurements, using a photonics integrated circuit (PIC) consisting of two individual homodyne LDVs [9]. So far, not

#190785 - $15.00 USD Received 17 May 2013; revised 18 Jun 2013; accepted 18 Jun 2013; published 27 Jun 2013

many LDV PICs have been reported. Compared to the compact self-mixing technique [10], on-chip homodyne LDV technique has easy demodulation algorithms. The footprint of this chip is smaller than 5 mm^2. This dual-LDV PIC is realized on the silicon photonics platform using CMOS compatible technologies [11]. Silicon photonics has become very important in recent years to implement high bandwidth transceivers for datacommunication applications. With this technology one can integrate passive optical waveguides, optical filters, optical modulators, optical detectors and optical sources on a silicon-on-insulator (SOI) wafer and do so with the standard technology portfolio of an advanced CMOS fab. But recently the same technology has also gained considerable interest for sensing and biosensing applications [12]. The big strength of silicon photonics over other optical integration technologies is that one can make use of the very mature toolset in an existing infrastructure and that there is a direct route to volume manufacturing at low cost.

In the following part, the working principle of the proposed dual-LDV system is demonstrated first. Then we discuss the algorithm for the PWV measurement, especially the cross-correlation method. The measurement results, including the calibration measurements of the dual-LDV PIC and a number of *in-vivo* PWV measurements, are demonstrated afterwards.

2. Description of the dual-LDV PIC

A detailed explanation to the principle of an on-chip single-point homodyne LDV has been given in [9]. The PIC-based PWV measurement device proposed in this paper consists of two such homodyne LDVs. The schematic of the on-chip system and the measurement setup is shown in Fig. 1(a). Despite the capability of integrating lasers and photo-detectors (PDs) on SOI chips [13, 14], we still use external laser and PDs in this proof-of-concept setup to solely test the performance of the passive optical system. The light source and the PDs are connected with the chip via a fiber array (FA), in which 12 single-mode fibers (2 meter long, core/cladding = 9/125 μm) have one of their ends assembled on a V-groove array with a pitch of 127 μm.

During the operation, coherent light generated in the external laser is sent to the chip via the FA. An optimized optical coupling between the fiber and the on-chip grating coupler (GC) is ensured by a polarization controller (*PC*). In the 1×4 optical splitter (*os1*) light is split into four parts: two parts are sent to the measurement arms of the two stand-alone LDVs, the third part

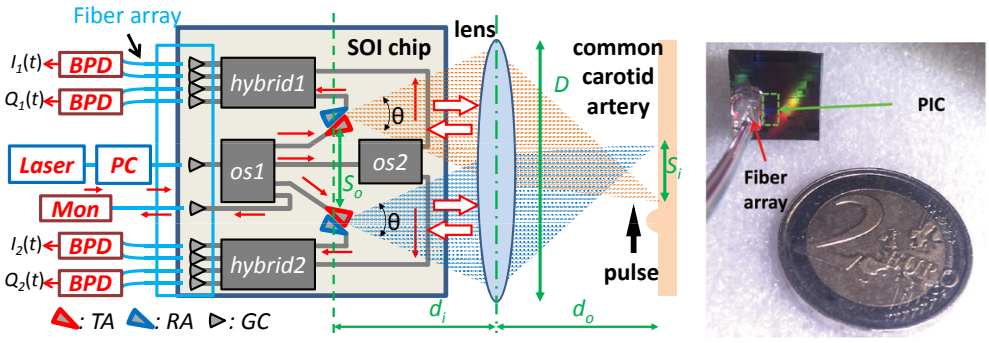

(a) (b)

Fig. 1. (a) The schematic of the PWV measurement device using a dual-LDV PIC chip. In the figure *os* (in *os1* and *os2*) stands for optical splitter, *hybrid* for 90° optical hybrid, *PC* for polarization controller, *BPD* for balanced photo-detectors, *Mon* for monitor, *TA* for transmitting antenna, *RA* for receiving antenna , *GC* for grating coupler. (b) The photo of a real dual-LDV chip with a bonded fiber array, compared with a two euro coin.

#190785 - $15.00 USD Received 17 May 2013; revised 18 Jun 2013; accepted 18 Jun 2013; published 27 Jun 2013

is split again into two reference signals with another optical splitter (*os2*), and the fourth part is directly sent out to a detector (*Mon* in Fig. 1(a)) to track the variations of the light intensity. Two light transmitting antennas (TAs) and two light receiving antennas (RAs), realized by means of grating couplers, are set in the measurement arms to send light out of the chip and receive back reflections, respectively. A lens is set in front of the chip to focus the two light beams from the TAs onto two locations on the neck region of the CCA. The two TAs (or RAs) have a separation S_o = 0.98 mm to ensure an adequate large distance S_i between the two measurement positions, which can be calculated as follows

$$S_i = |M|S_o = \left| -\frac{d_o}{d_i} \right| S_o, \tag{1}$$

where M is the magnification of the optical system, d_o and d_i are the object and image distances, respectively. The back-scattered signals are collected by the same lens and focused back to the chip, where they are picked up by the RAs. To ensure that enough reflection is coupled to their corresponding RAs, the locations of the RAs are set very close the TAs. According to the Doppler effect, the recaptured reflection signals carry the information of the vibrations in their time-dependent frequency shifts. They are mixed with the reference signals in the two 90° optical hybrids [15] (see Fig. 1(a)). From each 90° optical hybrid, four optical signals are obtained and sent to two external balanced PDs. The footprint of this PIC is smaller than 5 mm^2, and most of the space is taken by the FA. A photo of the chip is shown in Fig. 1(b), in which the actual area of the dual-LDV PIC is shown in the green box.

With the help of an analog-to-digital converter (ADC), the generated photocurrents of the balanced PDs are transformed into digital signals, which are used to recover the instantaneous velocity of each vibration using a digital "arc-tangent" demodulation method [9]. After the demodulation, two curves representing the instantaneous velocities of the vibrations can be obtained. The sampling time of the ADC t_s determines the maximal detectable displacement speed of the neck surface $v_m = \lambda_0/2t_s$, where λ_0 is the wavelength of the light. In our measurement, the sampling frequency $f_s = 1/t_s$ is chosen to be 40 kHz, which corresponds to a v_m of 31 mm/s. Note that the value v_m is not related to PWV.

Considering the resolution of a measured PWV, it is better to use a large S_i value, which is, however, limited by the size of the neck. In practice, the distance S_i is normally chosen to be larger than 1 cm, indicating that the value of $|M|$ is normally larger than 10. In this case, however, the numerical aperture of the lens on the image side is very small, which results in a strong reduction in the power of the backscattered light. In order to obtain a stronger reflection, two pieces of retro-reflective tapes are attached on the sites where the vibrations are measured. Considering the source side of the lens, the aperture of the lens D should be large enough to collect both light beams from the chip to avoid additional loss, indicating that $D > D_c = S_o + 2d_o \tan(\theta/2)$, where $\theta \simeq 11^\circ$ is the divergence angle of the output light (see Fig. 1(a)) and D_c is the total size of the two beams when they reach lens. In this setup, a lens (C280TME-C from Thorlabs) with a focal length f = 18.4 mm and aperture D = 5.5 mm is used, and its position is adjusted with the help of a translation stage. The separation S_i is around 1.5 cm, which leads to d_o = 300 mm and D_c = 4.8 mm (being smaller than D).

Since optical frequency shifters are not used in homodyne LDVs (see [16]), homodyne LDVs have a relatively low production cost compared to heterodyne. Hence homodyne LDVs are used in this device. However, homodyne LDVs also have drawbacks, e.g. they may not work well for vibrations smaller than half a wavelength. But this problem is not critical in the PWV measurement and can be alleviated by stabilizing the laser source and using a temperature controller. In addition, the wave pulse is usually very strong and thus weaker vibrations can usually be ignored.

#190785 - $15.00 USD Received 17 May 2013; revised 18 Jun 2013; accepted 18 Jun 2013; published 27 Jun 2013

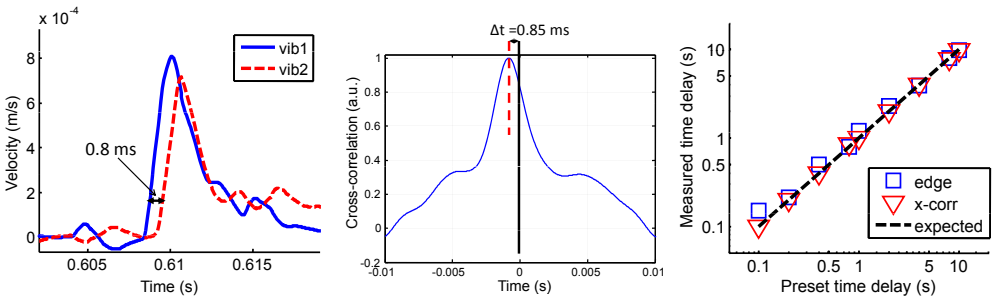

(a) (b) (c)

Fig. 2. Calibration measurement results of two pulses generated on two separate earphones. The two pulses are with similar shapes but are generated at different times. (a) The measured two pulses with a delay of 0.8 ms. (b) The cross correlation of the two velocity curves, which shows a time delay of 0.85 ms. (c) The recovered delay time for different method, where *x-corr* means cross-correlation method.

3. Algorithms for retrieving PWV

The PWV is usually retrieved by measuring the transit time of the pulse wave between the two measurement locations, denoted as Δt. The value of PWV can be obtained from Δt and S_i using the following formula

$$PWV = S_i/\Delta t. \tag{2}$$

The accuracy of the PWV measurement thus depends on the accuracy of the retrieved transit time Δt. The maximal detectable PWV value PWV_m is ultimately limited by the sampling frequency t_s of ADC, and their relation can be written as $PWV_m = S_i/t_s$. Providing f_s = 40 kHz and S_i = 1.5 cm, a PWV_m of 600 m/s can be obtained. However, due to the inaccuracy in the algorithm for retrieving Δt and deviations in the measurements, the PWV_m is determined by the transit-time error t_d in the measurement rather than t_s. The value t_d depends on many factors, including shape changes between the two pulses, errors in the LDV outputs due to the weak useful reflection and the existence of on-chip spurious reflections, and limitations in the algorithms used for retrieving Δt. In [3], a cross-correlation algorithm is used to retrieve the PWV, in which the transit time between the two measurement locations (Δt) is obtained from the cross-correlation of the two measured velocity curves. The accuracy of this method depends on the shape changes between the measured velocity curves of the two vibrations. These shape changes are partly caused by propagation dispersion of the pulse wave and reflection at sites with impedance mismatch [6], and partly caused by errors of homodyne LDVs when light reflection is not strong enough. Hermeling *et al*. proposed to use the transit time of the systolic foot of the pressure waveform [6], in which the deviation also depends on the shape variation and the accuracy of the LDV system. However, this algorithm is more complex than the cross-correlation method in many cases.

4. Measurement results

The LDV PICs are fabricated via ePIXfab [17]. A calibration measurement was firstly done on two separate earphones, on which two pulses were generated by two voltage signals with the same shape but a relative preset time delay Δt. The input light with a wavelength of 1550 nm has a power of 6 dBm and linewidth of 150 kHz. Light at this wavelength has the minimal loss in both optical fibers and SOI devices. These challenging test conditions correspond to a pulse

#190785 - $15.00 USD Received 17 May 2013; revised 18 Jun 2013; accepted 18 Jun 2013; published 27 Jun 2013

wave velocity of up to 150 m/s, which is well beyond the values that can be expected *in vivo*. In Fig. 2(a), the velocity curves of the two pulses with a preset delay Δt = 0.8 ms is shown. It can be seen that a time delay of 0.8 ms is retrieved from the leading edge delay of two pulses, while the delay derived from the cross-correlation method is around 0.85 ms (see Fig. 2(b)). The retrieved results of these two methods have been compared using a series of measurements (see Fig. 2(c)). The measured root-mean-square deviations of the leading-edge and cross-correlation algorithms are 0.13 ms and 0.08 ms, respectively. The cross-correlation method is less sensitive to noise and spurious reflections in this situation. Besides, their influences are also strongly reduced by filtering. Therefore, the estimated deviation is mainly caused by the shape difference between the two pulses.

Then the device was used to measure the CCA PWV *in vivo*. The person under test was a healthy male volunteer aged 26 years. During the test, the volunteer was sitting in an upright position in front of the device, with two retro-reflective tapes attached to two locations along the CCA (see Fig. 3). The separation of the two locations was between 1.5 cm and 1.7 cm. The two light beams were adjusted to be focused on the two retro-reflective tapes, respectively. The demodulated velocity results for a representative measurement are shown in Fig. 4(a), and the cross-correlation of the velocities is obtained and shown in Fig. 4(b). It is seen that the transit time of the pulse is around 3.3±0.1 ms, and this corresponds to a PWV between 4.85±0.45 m/s. The displacement and acceleration signals are also shown in Fig. 5(a) and Fig. 5(b). If a proper filter is applied, the cross-correlation method can also work well with the acceleration signal, but not with the displacement signal, which has a strong low-frequency variation. Another byproduct of the LDV system is the heart rate of the subject. In this measurement, the average

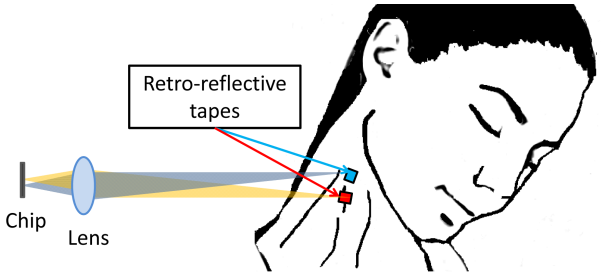

Fig. 3. Schematic of the CCA PWV measurement using on-chip dual-LDV system.

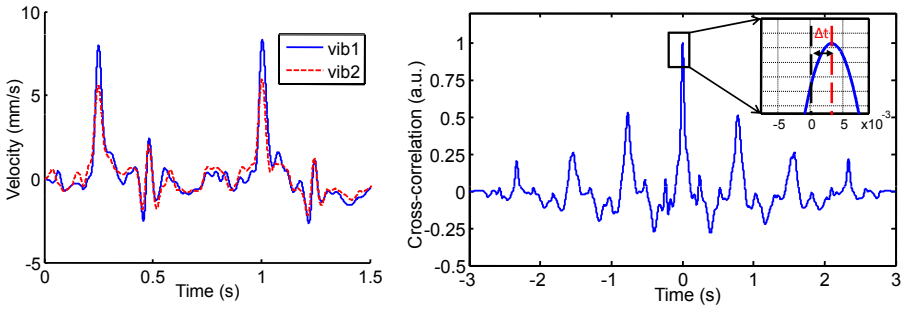

(a) (b)

Fig. 4. (a) The velocity curves of the two pulses. (b) The cross-correlation of the two measured pulses. A time delay Δt = 3.3 ms is obtained using the correlation method.

#190785 - $15.00 USD Received 17 May 2013; revised 18 Jun 2013; accepted 18 Jun 2013; published 27 Jun 2013

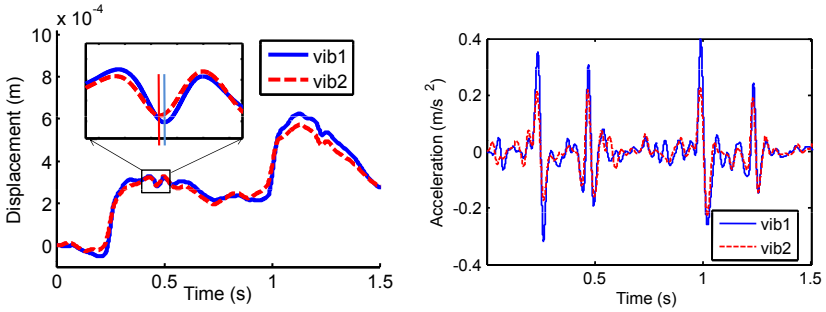

(a) (b)

Fig. 5. (a) The displacements of the two pulses. (b) The accelerations of the two pulses.

heart rate of the subject is around 78 bpm, which is calculated according to the time delay between two adjacent pulses.

5. Conclusion

In this paper, the proof-of-concept of a miniaturized PWV measurement device utilizing dual-LDV photonic integrated circuit is demonstrated with initial experimental results. The cross-correlation method is used to derive the PWV, and the time delay error was found to be 0.1 ms. When the separation between the two measurement spots is only 1.5 cm apart from each other, the measurable range of this device can cover all possible values of the CCA PWV. In future work, efforts should be made to integrate lasers and photo-detectors on the same photonic integrated circuits. A PIC with more than two LDVs is also interesting for future study since it can be used to obtain more information of the pulses at different locations.

Acknowledgments

The authors acknowledge the Ghent University-Methusalem project “Smart Photonic Chips” for financial supports. The authors thank Ruijun Wang, and Lianyan Li for useful discussions.

#190785 - $15.00 USD Received 17 May 2013; revised 18 Jun 2013; accepted 18 Jun 2013; published 27 Jun 2013